Laser and Particle Beams (2014), *32*, 657–663.

doi:10.1017/S0263034614000688

Study of coexisting stimulated Raman and Brillouin scattering at relativistic laser power

ASHISH VYAS, RAM KISHOR SINGH, AND R.P. SHARMA
Centre for Energy Studies, IIT Delhi, India
(Received 29 May 2014; Accepted 7 October 2014)

Abstract

This paper presents a model to study the stimulated Raman scattering (SRS) and stimulated Brillouin scattering (SBS) simultaneously at relativistic laser power. At high intensity, the relativistic mass correction for the plasma electrons becomes significant and the plasma refractive index gets modified which leads to the relativistic self-focusing of the pump beam. This filamentation process affects the scattering processes (SRS and SBS) and at the same time the pump filamentation process also gets modified in the presence of the coexisting SRS and SBS due to the pump depletion. We have also demonstrated that the pump depletion and relativistic filamentation affects the back-reflectivity of scattered beams (SRS and SBS) significantly, for the coexistence case.

Keywords: Relativistic nonlinearity; Self-focusing; Stimulated Brillouin scattering; Stimulated Raman scattering

1. INTRODUCTION

Due to availability of the high power lasers, laser plasma interaction at higher intensity (10^{18}–10^{21} W/cm^2) becomes an important nonlinear phenomenon in recent years. The propagation of an intense laser beam through the plasma results into various instabilities namely, self-focusing, filamentation, stimulated Raman scattering (SRS), stimulated Brillouin scattering (SBS), two plasmon decay, etc. (Krall *et al.*, 1973; Kruer, 1974; Liu *et al.*, 1994; Guérin *et al.*, 1998). These instabilities play a very important role in many areas like fast-ignitor thermonuclear fusion (Deutsch *et al.*, 1996), compact laser-driven accelerators (Tajima *et al.*, 1979), X-ray lasers (Li *et al.*, 2011), laboratory astrophysics (Remington *et al.*, 1999), and many more (Tajima *et al.*, 2002), where laser plasma interaction takes place. In particular, SRS corresponds to the decay of the incident electromagnetic wave into a scattered electromagnetic wave and an electron plasma wave (EPW), while during SBS the incident electromagnetic wave decays into a scattered electromagnetic wave and an ion acoustic wave (IAW). In this paper, we are mainly concerned about SRS and SBS because due to these instabilities, a large fraction of the high power laser energy is not efficiently coupled with plasma as well as modification of the intensity distribution takes place which affect the uniformity of energy deposition (Kruer, 1974; Liu *et al.*, 1994; Lindl *et al.*, 2004; Omatsu *et al.*, 2012). Apart from SRS and SBS, the self-focusing of the laser beam is also a crucial problem in high power laser plasma interactions. For the propagation of a nonuniform intense laser beam inside the plasma, both ponderomotive nonlinearity and relativistic nonlinearity can lead to the self-focusing process. The relativistic self-focusing occurs because at such higher intensities the field associated with the light wave becomes very high which accelerates the plasma electrons at relativistic velocities and hence the relativistic mass correction must be taken into account. This relativistic change in the electron mass modifies the dielectric constant of plasma $\varepsilon = 1 - \omega_{pe}^2/\gamma\omega_0^2$, where $\omega_{pe} = (4\pi N_e e^2/m_0)^{1/2}$ is the plasma frequency, ω_0 is the laser frequency, N_e is the plasma electron density, e and m_0 are the charge and rest mass of the electron, respectively, and γ is the relativistic Lorentz factor. Therefore, plasma refractive index ($\sqrt{\varepsilon}$) seen by the intense laser beam becomes γ dependent which leads to the relativistic self-focusing and breakup of the laser beam into intense filaments (Umstadter, 2003). On the other hand, ponderomotive nonlinearity modifies the refraction index by expulsion of the electrons from the higher intensity region. However, these nonlinearities are operative at different time scales according to the inequalities (1) $\tau < \tau_{pe}$ or (2) $\tau_{pe} < \tau < \tau_{pi}$; here, τ is laser pulse duration, τ_{pe} is the electron plasma period, and τ_{pi} is ion plasma period. In case (1), the relativistic nonlinearity is set up (almost instantaneously) while for case (2), both the nonlinearities (relativistic and

Address correspondence and reprint requests to: Ashish Vyas, Centre for Energy Studies, IIT Delhi, India 110016. E-mail: ashishvyas.optics@gmail.com

ponderomotive) are operative (Brandi *et al.*, 1993). So, relativistic nonlinearity will set up almost instantaneously in the system and requires relatively higher threshold laser power than the ponderomotive nonlinearity (Brandi *et al.*, 1993). This relativistic nonlinearity (self-focusing) creates a hindrance in uniform energy deposition of the laser inside the plasma. So both SRS and SBS along with the relativistic self-focusing greatly affect the laser plasma coupling. Relativistic self-focusing occurs when the laser power exceeds the critical (threshold) power, given by $P_c = 17\gamma(\omega_0/\omega_{pe})^2$GW (Sun *et al.*, 1987; Sprangle *et al.*, 1987), which is available for experiments due to the recent advancement in laser technology. Therefore, these instabilities at high power laser flux have been very actively studied experimentally (Monot *et al.*, 1995; Borghesi *et al.*, 1997; Wang *et al.*, 2000; Rousseaux *et al.*, 2002).

In the past, a lot of theoretical and numerical works at high power laser flux has been done in which SRS and SBS are carried out separately (three wave interaction = 3WI), ignoring the interplay among them (Guérin *et al.*, 1995; Barr *et al.*, 1998; Mahmoud *et al.*, 2001; Shuller *et al.*, 2010; Paknezhad *et al.*, 2012). However, SRS and SBS can coexist upto $N_{cr}/4$ inside the plasma (SRS exists upto $N_{cr}/4$ while SBS exists upto N_{cr}) (Kruer, 1974; Liu *et al.*, 1994), where N_{cr} is the electron critical density, defined as the density above which the propagation of the electromagnetic wave is not allowed. Although, the interplay between SRS and SBS has been theoretically studied earlier (Kolber *et al.*, 1995; Sharma *et al.*, 2013; Hao *et al.*, 2013). Recently, Sharma *et al.* (2013) have studied the effect of ponderomotive nonlinearity on coexisting stimulated Raman and Brillouin scattering, but these studies are carried out at relatively low powers. Therefore, not applicable at ultra-intense laser plasma interaction where the relativistic nonlinearity plays a very important role. In order to understand the interplay among SRS and SBS at relativistic laser power, it is essential to study these instabilities along with the relativistic self-focusing in the regime where they co-exist and affect each other.

The interplay between SRS and SBS has been observed in many experiments (Walsh *et al.*, 1984; Labaune *et al.*, 1997; Michel *et al.*, 2010). The first experimental observation of this competitive phenomenon was made by Walsh *et al.* (1984) in which they observed that the quenching of SRS plasma waves were strongly correlated to the initiation of SBS ion waves. Recently, it has been found experimentally that for plasma based laser amplifiers, it is essential to study SRS and SBS simultaneous at relativistic laser power (Turnbull *et al.*, 2012; Weber *et al.*, 2013). Therefore, the motivation of the present work is to understand the effect of the coexistence on the growth, saturation, and the reflectivity of SRS and SBS including the effect of relativistic self-focusing of intense Gaussian laser beam.

This paper presents the simultaneous study of stimulated Raman and Brillouin scattering along with the effect of relativistic filamentation of the pump beam within the paraxial-ray approximation. The back reflectivity is a very important parameter to assure the amount of energy dissipated in laser plasma interaction therefore we have simulated the back-reflectivity of the scattered waves (SRS and SBS) and studied how it gets modified due to this coexistence process. We have also examined how the pump depletion affects the filamentation process (of the pump beam as well as scattered beams) and the back reflectivity of scattered beams. It has been demonstrated that the relativistic filamentation modifies the SRS and SBS gain parameters which further modifies the back-reflectivities of the scattered beams.

This paper is arranged as follows. In Section 2, we have described a three-dimensional theoretical model to study the effect of relativistic filamentation of the pump on the coexistence of SRS and SBS and derived the expression for SRS and SBS back-reflectivity. Section 3 presents the detailed discussion of the results followed by the conclusion in Section 4.

2. MODEL EQUATION

In this section, we have developed a five wave interaction (5WI) model to study the interplay between SRS and SBS at relativistic laser power. A high power laser beam with Gaussian intensity profile is treated as the pump which is polarized along the *x*-axis and propagating along the *z*-axis in collisionless plasma. The expression of the initial intensity distribution along the wave front is given by:

$$\vec{E}_0.\vec{E}_0^*|_{Z=0} = E_{00}^2 \exp(-r^2/r_0^2), \quad (1)$$

where r_0 is the initial beam width, E_{00} is the axial amplitude, and r refers to the radial coordinate in cylindrical co-ordinate system. To study the coexistence case, we are mainly concern about the coupling of three fields — the incident pump field $\vec{E}_0$, the Raman backscattered field $\vec{E}_R$, and the Brillouin backscattered field $\vec{E}_B$. Following the standard technique used by Sharma *et al.* (2013) including the relativistic mass correction, one can obtain the following governing equations for the pump and scattered fields:

$$\nabla^2 E_0 + \frac{\omega_0^2}{c^2}\left[1 - \frac{\omega_{pe}^2}{\gamma\omega_0^2}\right]E_0 = \frac{-4\pi e}{c^2}\frac{1}{2}\frac{\partial}{\partial t}(N_{eR}V_R + N_{eB}V_B), \quad (2)$$

$$\nabla^2 E_R + \frac{\omega_R^2}{c^2}\left[1 - \frac{\omega_{pe}^2}{\gamma\,\omega_R^2}\right] E_R = \frac{-4\,\pi\,e}{c^2}\frac{1}{2}\frac{\partial}{\partial t}(N_{eR}^* V_0), \quad (3)$$

$$\nabla^2 E_B + \frac{\omega_B^2}{c^2}\left[1 - \frac{\omega_{pe}^2}{\gamma\,\omega_B^2}\right]E_B = \frac{-4\,\pi\,e}{c^2}\frac{1}{2}\frac{\partial}{\partial t}(N_{eB}^* V_0), \quad (4)$$

where γ is the relativistic Lorentz factor and other symbols have their usual meanings. Here N_{eR} and N_{eB} are the electron density perturbations in the EPW and IAW, respectively.

Using the heavy damping limit one can obtain:

$$\frac{N_{eR}}{N_0} \approx i\frac{e^2 k_L^2 E_0.E_R^*}{4\, m_0^2\, \gamma^2 \Gamma_e\, \omega_L\, \omega_0 \omega_R}, \tag{5}$$

$$\frac{N_{eB}}{N_0} \approx i\frac{e^2 \omega_A E_0.E_B^*}{4 m_0 \gamma M \Gamma_i \omega_0 \omega_B c_s^2}, \tag{6}$$

where Γ_e and Γ_i are the Landau damping coefficients for EPW and IAW, respectively, T_e and T_i are electron and ion temperatures, k_β is the Boltzmann's constant, and λ_d is the Debye length. Using Eqs (5) and (6), the following equations are obtained:

$$\nabla^2 E_0 + \frac{\omega_0^2}{c^2}\left[1 - \frac{\omega_{pe}^2}{\gamma\,\omega_0^2}\right] E_0 = \omega_{pe}^2\left[\frac{ie^2 k_L^2 |E_R.E_R^*|}{8\, m_0^2\, \gamma^3\, \omega_L\, \omega_R^2 c^2\, \Gamma_e}\right] E_0 + \omega_{pe}^2\left[\frac{ie^2 \omega_A |E_B E_B^*|}{8 m_0 M\, \gamma^2 \Gamma_i c_s^2 c^2 \omega_B^2}\right] E_0, \tag{7}$$

$$\nabla^2 E_R + \frac{\omega_R^2}{c^2}\left[1 - \frac{\omega_{pe}^2}{\gamma \omega_R^2}\right] E_R = \omega_{pe}^2\left[\frac{e^2 k_L^2 |E_0.E_0^*|}{8 i m_0^2 \gamma^3 \omega_L \omega_0^2 c^2 \Gamma_e}\right] E_R, \tag{8}$$

$$\nabla^2 E_B + \frac{\omega_B^2}{c^2}\left[1 - \frac{\omega_{pe}^2}{\gamma \omega_B^2}\right] E_B = \omega_{pe}^2\left[\frac{e^2 \omega_A |E_0 E_0^*|}{8 i m_0 \gamma^2 M c_s^2 c^2 \omega_0^2 \Gamma_i}\right] E_B \tag{9}$$

One can solve Eqs (7), (8), and (9) by using the paraxial ray approximation. Writing

$$E_0 = A_{00}(r, z)\ \exp\{-ik_0(z + S_0(r, z))\}, \tag{10}$$

$$E_R = A_{R0}(r, z)\ \exp\{-ik_R(z + S_R(r, z))\}, \tag{11}$$

$$E_B = A_{B0}(r, z)\ \exp\{-ik_B(z + S_B(r, z))\}. \tag{12}$$

Using the above equations in Eqs (7), (8), and (9) and on separating real and imaginary parts, one can obtain a set of coupled equations. Eq. (7) gives (Akhmanov *et al.*, 1968)

$$2\frac{\partial A_{00}}{\partial z} + 2\frac{\partial A_{00}}{\partial r}\frac{\partial S_0}{\partial r} + \left(\frac{\partial^2 S_0}{\partial r^2} + \frac{1}{r}\frac{\partial S_0}{\partial r}\right) A_{00} + e^2 \omega_{pe}^2\left[\frac{k_L^2 |A_{R0}|^2}{8 m_0^2 \gamma^3 \omega_L \omega_0 \omega_R^2 \Gamma_e c \varepsilon_0^{1/2}} + \frac{\omega_A |A_{B0}|^2}{8 m_0 M \gamma^2 \Gamma_i c_s^2 \omega_B^2 \omega_0 c \varepsilon_0^{1/2}}\right] A_{00}^2 = 0, \tag{13}$$

and

$$2\frac{\partial S_0}{\partial z} + \left(\frac{\partial S_0}{\partial r}\right)^2 = \frac{\omega_{pe}^2}{\omega_0^2}\left(\frac{\gamma - 1}{\gamma \varepsilon_0}\right) + \frac{1}{k_0^2 A_{00}}\left(\frac{\partial^2 A_{00}}{\partial r^2} + \frac{1}{r}\frac{\partial A_{00}}{\partial r}\right) \tag{14}$$

similarly, Eq. (8) gives:

$$2\frac{\partial A_{R0}}{\partial z} + 2\frac{\partial A_{R0}}{\partial r}\frac{\partial S_R}{\partial r} + \left(\frac{\partial^2 S_R}{\partial r^2} + \frac{1}{r}\frac{\partial S_R}{\partial r}\right) A_{R0} - e^2 \omega_{pe}^2\left[\frac{k_L^2 |A_{00}|^2}{8\, m_0^2\, \gamma^3\, \omega_L\, \omega_0^2 \omega_R\, \Gamma_e c \varepsilon_R^{1/2}}\right] A_{R0} = 0 \tag{15}$$

and

$$2\frac{\partial S_R}{\partial z} + \left(\frac{\partial S_R}{\partial r}\right)^2 = \frac{\omega_{pe}^2}{\omega_R^2}\left(\frac{\gamma - 1}{\gamma \varepsilon_R}\right) + \frac{1}{k_R^2 A_{R0}}\left(\frac{\partial^2 A_{R0}}{\partial r^2} + \frac{1}{r}\frac{\partial A_{R0}}{\partial r}\right), \tag{16}$$

similarly, Eq. (9) gives:

$$2\frac{\partial A_{B0}}{\partial z} + 2\frac{\partial A_{B0}}{\partial r}\frac{\partial S_B}{\partial r} + \left(\frac{\partial^2 S_B}{\partial r^2} + \frac{1}{r}\frac{\partial S_B}{\partial r}\right) A_{B0} - e^2 \omega_{pe}^2\left[\frac{\omega_A |A_{00}|^2}{8 m_0 M \gamma^2 \Gamma_i c_s^2 \omega_0^2 \omega_B c \varepsilon_B^{1/2}}\right] A_{B0} = 0 \tag{17}$$

and

$$2\frac{\partial S_B}{\partial z} + \left(\frac{\partial S_B}{\partial r}\right)^2 = \frac{\omega_{pe}^2}{\omega_B^2}\left(\frac{\gamma - 1}{\gamma \varepsilon_B}\right) + \frac{1}{k_B^2 A_{B0}}\left(\frac{\partial^2 A_{B0}}{\partial r^2} + \frac{1}{r}\frac{\partial A_{B0}}{\partial r}\right). \tag{18}$$

The solution for the pump wave (Eqs (13) and (14)) can be written as (Akhmanov *et al.*, 1968)

$$A_{00}^2 = \frac{E_{00}^2(z=0)}{f_0^2(z)} \exp\left[-\frac{r^2}{r_0^2\, f_0^2(z)} - 2G_0 z\right], \tag{19}$$

$$S_0 = \frac{r^2}{2}\frac{1}{f_0(z)}\frac{df_0(z)}{dz} + \Phi_0(z), \tag{20}$$

$$G_0 = e^2 \omega_{pe}^2 \left[\frac{k_L^2 |A_{R0}|_{r=0}^2}{16\, m_0^2\, \gamma^3\, \omega_L\, \omega_0 \omega_R^2\, \Gamma_e c\, \varepsilon_0^{1/2}} + \frac{\omega_A |A_{B0}|_{r=0}^2}{16\, m_0 M\, \gamma^2\, \Gamma_i c_s^2\, \omega_B^2 \omega_0\, c\, \varepsilon_0^{1/2}}\right]. \tag{21}$$

https://doi.org/10.1017/S0263034614000688 Published online by Cambridge University Press

Similarly, the following solutions are obtained for the Raman scattered beam (Eqs (15) and (16)):

$$A_{R0}^2 = \frac{E_{R0}^2(z'=0)}{\mathrm{f}_R^2(z')}\exp\left[-\frac{r^2}{r_R^2\,\mathrm{f}_R^2(z')} - 2g_R z'\right], \tag{22}$$

$$S_R = \frac{r^2}{2}\frac{1}{\mathrm{f}_R(z')}\frac{d\mathrm{f}_R(z')}{dz} + \Phi_R(z'), \tag{23}$$

$$g_R = -e^2\omega_{pe}^2\left[\frac{k_L^2|A_{00}|_{r=0}^2}{16\,m_0^2\,\gamma^3\,\omega_L\,\omega_0^2\omega_R\,\Gamma_e c\varepsilon_R^{1/2}}\right]. \tag{24}$$

Here $z' = L_z - z$, L_z is the interaction length. Similarly, the solutions for the Brillouin scattered beam (Eqs (17) and (18)) are:

$$A_{B0}^2 = \frac{E_{B0}^2(z'=0)}{\mathrm{f}_B^2(z')}\exp\left[-\frac{r^2}{r_B^2\mathrm{f}_B^2(z')} - 2g_B z'\right], \tag{25}$$

$$S_B = \frac{r^2}{2}\frac{1}{\mathrm{f}_B(z')}\frac{d\mathrm{f}_B(z')}{dz} + \Phi_B(z'), \tag{26}$$

$$g_B = -e^2\,\omega_{pe}^2\left[\frac{\omega_A\,|A_{00}|_{r=0}^2}{16\,m_0 M\,\gamma^2\,\Gamma_i c_s^2\,\omega_0^2\,\omega_B c\,\varepsilon_B^{1/2}}\right]. \tag{27}$$

Here G_0, g_R and g_B are the gain factors for the pump wave, SRS wave and SBS wave, respectively, in 5WI case and other symbols have their usual meaning. Here the relativistic factor γ is given by

$$\gamma = \left[1 + \frac{\alpha_0 E_{00}^2}{\mathrm{f}_0^2(z)}\exp\left(\frac{-r^2}{r_0^2\mathrm{f}_0^2(z)} - 2G_0 z\right) + \frac{\alpha_R E_{R0}^2}{\mathrm{f}_R^2(z')}\exp\left(\frac{-r^2}{r_R^2\mathrm{f}_R^2(z')} - 2g_R z'\right) + \frac{\alpha_B E_{B0}^2}{\mathrm{f}_B^2(z')}\exp\left(\frac{-r^2}{r_B^2\mathrm{f}_B^2(z')} - 2g_B z'\right)\right] \tag{28}$$

where

$$\alpha_{0,R,B} = \frac{e^2}{m_0^2 c^2\omega_{0,R,B}^2}. \tag{29}$$

Here f_0, f_R and f_B are the dimensionless beam width parameters of the pump beam , SRS and SBS beam, respectively. The governing differential equations for the dimensionless beam width parameters are given by:

$$\frac{d^2\mathrm{f}_0}{dz^2} = \frac{1}{k_0^2\,r_0^4\,\mathrm{f}_0^3} - \frac{\omega_{pe}^2}{\omega_0^2\varepsilon_0}\mathrm{f}_0\,\beta, \tag{30}$$

$$\frac{d^2\mathrm{f}_R}{dz'^2} = \frac{1}{\mathrm{k}_R^2 r_R^4\mathrm{f}_R^3} - \frac{\omega_{\mathrm{pe}}^2}{\omega_\mathrm{R}^2\varepsilon_R}\mathrm{f}_R\beta, \tag{31}$$

$$\frac{d^2\mathrm{f}_B}{dz'^2} = \frac{1}{\mathrm{k}_B^2 r_B^4\mathrm{f}_B^3} - \frac{\omega_{\mathrm{pe}}^2}{\omega_\mathrm{B}^2\varepsilon_B}\mathrm{f}_B\beta, \tag{32}$$

where β is given by

$$\beta = \frac{1}{2}\left[\frac{\alpha_0 E_{00}^2}{r_0^2\mathrm{f}_0^4(z)}\exp(-2G_0 z) + \frac{\alpha_R E_{R0}^2}{r_R^2\mathrm{f}_R^4(z')}\exp\left(-2g_R z'\right) + \frac{\alpha_B E_{B0}^2}{r_B^2\mathrm{f}_B^4(z')}\exp\left(-2g_B z'\right)\right] \times\left[1 + \frac{\alpha_0 E_{00}^2}{\mathrm{f}_0^2(z)}\exp(-2G_0 z) + \frac{\alpha_R E_{R0}^2}{\mathrm{f}_R^2(z')}\exp\left(-2g_R z'\right) + \frac{\alpha_B E_{B0}^2}{\mathrm{f}_B^2(z')}\exp\left(-2g_B z'\right)\right]^{-3/2}. \tag{33}$$

In order to see the effect of filamentation on the backscattered beams, we have derived the expression of the back reflectivity for the SRS wave and the SBS wave:

$$R_{SRS} = \frac{|E_R E_R^*|}{E_{00}^2}v_{gr} = \frac{E_{R0}^2(z'=0)}{E_{00}^2}\frac{v_{gr}}{\mathrm{f}_R^2(z')}\mathrm{e}^{-2g_R z'}, \tag{34}$$

$$R_{SBS} = \frac{|E_B E_B^*|}{E_{00}^2} = \frac{E_{B0}^2(z'=0)}{E_{00}^2}\frac{1}{\mathrm{f}_B^2(z')}e^{-2g_B z'}, \tag{35}$$

where $v_{gr} = (1-\omega_{pe}^2/\omega_R^2)^{1/2}(1-\omega_{pe}^2/\omega_0^2)^{-1/2}$, is ratio of the group velocity of the SRS beam to the group velocity of the pump beam. In the next section the numerical results are obtained.

3. RESULTS AND DISCUSSION

By solving the set of coupled Eqs (30), (31), and (32); we can obtain the dynamical evolution of the pump beam (f_0) and the scattered beams (f_R and f_B). In these coupled equations; the first term (diffraction term) in the right-hand side leads to the divergence, while the second term (nonlinear coupling term) is responsible for the converging behavior of the respective beam. We have solved these coupled equations numerically by Runge-Kutta methods, for the parameter: $\frac{N_o}{N_{cr}} = 0.01$, $\lambda = 1.053\ \mu\mathrm{m}$, $r_0 = r_{R,B} = 12\ \mu\mathrm{m}$, $\mathrm{v}_{\mathrm{th}} = 0.1\mathrm{c}$, $I = 5\times10^{19}\ \mathrm{W/cm^2}$, Seed beam intesity $= I\times10^{-4}\ \mathrm{W/cm^2}$

https://doi.org/10.1017/S0263034614000688 Published online by Cambridge University Press

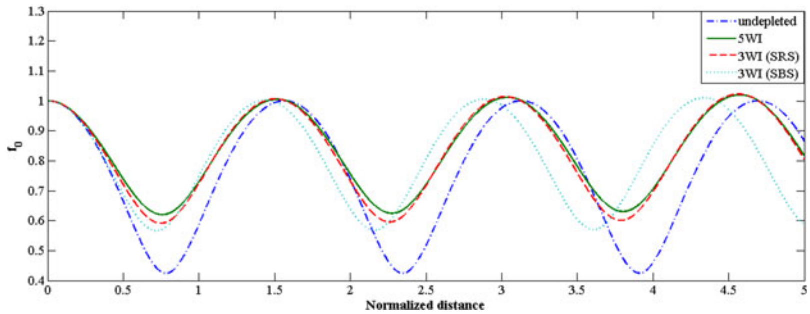

Fig. 1. Variation of the dimensionless beam width parameters for the pump beam with the normalized distance of propagation.

by using the following boundary conditions:

$$\mathrm{f}_0|_{z=0} = \mathrm{f}_R|_{z'=0} = \mathrm{f}_B|_{z'=0} = 1 \text{ and}$$
$$\left.\frac{d\mathrm{f}_0}{dz}\right|_{z=0} = \left.\frac{d\mathrm{f}_R}{dz'}\right|_{z'=0} = \left.\frac{d\mathrm{f}_B}{dz'}\right|_{z'=0} = 0.$$

Figure 1 shows the variation of the dimensionless beam width parameters of the pump beam (f_0) versus normalized distance of propagation for different cases. Dotdash curve corresponds to the undepleted pump case, dot and dash curve correspond to the pump depletion in isolated SBS and SRS, respectively, (3WI case) and solid curve depicts the pump depletion in 5WI case. Figure 2 represents the variation in the normalized intensity of the pump beam against the normalized distance of propagation for two cases: (1) corresponds to the undepleted pump case and; (2) corresponds to the pump depletion in 5WI case respectively. It is clear from the above figures that the relativistic filamentation process gets affected by the pump depletion significantly. Due to the pump depletion the relativistic Lorentz factor gets modified, which suppresses the filamentation. In the 5WI case, the pump depletion is more (in comparison to undepleted case and 3WI case) and hence results in lesser filamentation. Similarly, for the Raman and Brillouin back scattered beams, Figures 3a and 3b represents the normalized intensity variation respectively for the 5WI case. Intensities are normalized by the initial peak intensity of the pump beam.

The variation in the back reflectivity against the normalized distance of propagation for SRS and SBS processes is shown in Figures 4 and 5, respectively. For each process, two cases are considered, dash and dot-dash curve corresponds to the without filamentation case (also referred as plane pump wave case) whereas dot and solid curve corresponds to the filamentation case (also referred as Gaussian

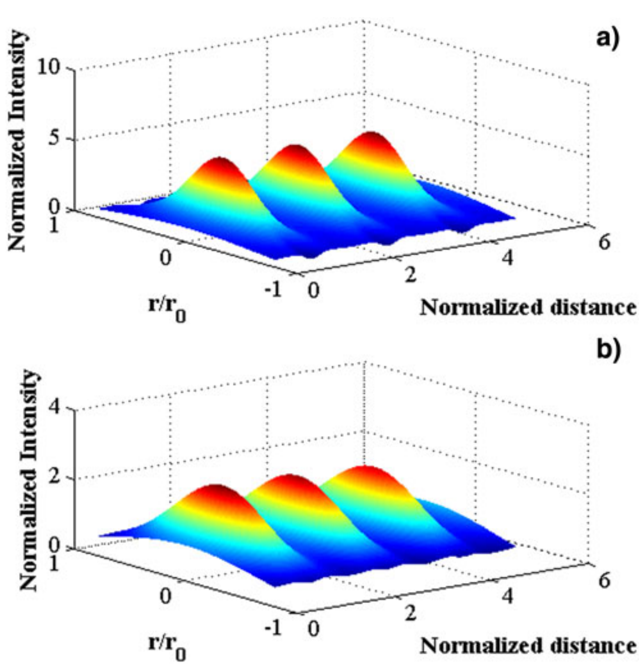

Fig. 2. Normalized intensity plot of pump laser beam (**a**) without depletion, and (**b**) with depletion (5WI case).

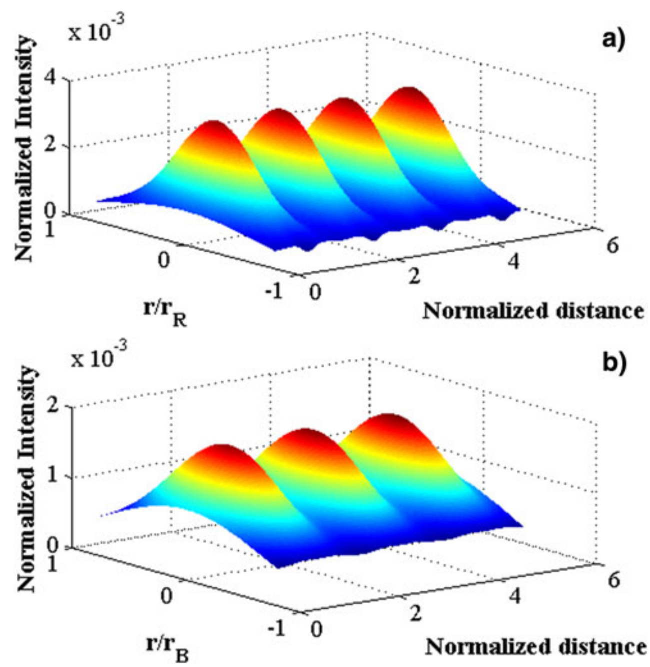

Fig. 3. Normalized Intensity plot of back scattered beams in five wave interaction case (**a**) SRS and (**b**) SBS.

https://doi.org/10.1017/S0263034614000688 Published online by Cambridge University Press

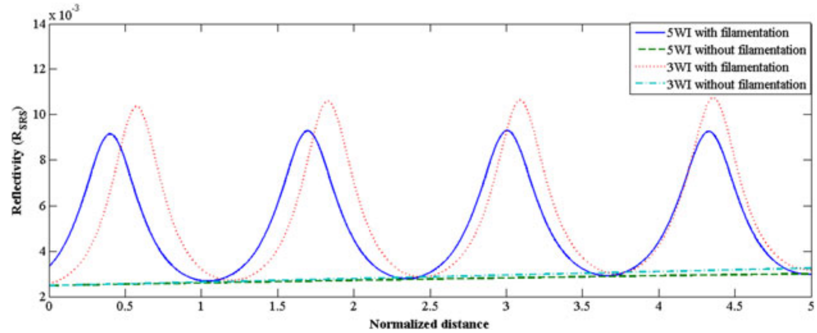

Fig. 4. The variation of back reflectivity of SRS process with the normalized distance of propagation.

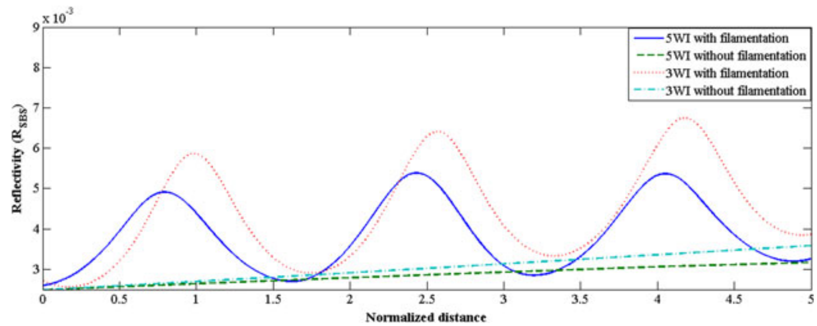

Fig. 5. The variation of back reflectivity of SBS process with the normalized distance of propagation.

pump wave case). Since the intensity of the scattered beams is proportional to the intensity of the pump, therefore enhancement in the back scattering is expected due to filamentation in contrast to the without filamentation case. Due to this filamentation effect, the intensity of the laser beam gets enhanced, which further modifies the gains (g_R and g_B) and consequently the back reflectivities (R_{SRS} and R_{SBS}) also get enhanced at the focused positions. In both the cases (filamentation and without filamentation), reflectivity for the 5WI case is always lower than 3WI case because the pump depletion in 5WI case is more than the 3WI case, which results in the lower reflectivity for the 5WI case.

Due to relativistic mass correction in the electron mass, modification in the back reflectivity for the SRS process (R_{SRS}) is expected however the back reflectivity for the SBS process (R_{SBS}) is not supposed to be changed. But from the Figure 5 it is clear that R_{SBS} is greatly affected by relativistic self-focusing process, which can be understood as follows: from the set of coupled Eqs. (30), (31), and (32) the dimensionless beam width parameter of the SBS beam (f_B) depends on coupling factor β, which further depends on the dimensionless beam width parameter (f_R) and gain (g_R) of the SRS beam along with the other parameters. In addition to this SBS gain factor g_B also depends on relativistic factorγ, which is a function of f_R and g_R along with the other parameters. So any modification in the SRS process due to relativistic mass correction will further affect the f_B and g_B, hence the R_{SBS} gets modified.

4. CONCLUSION

In summary, we have studied the two coexisting instabilities, SRS and SBS simultaneously, at relativistic laser power along with the relativistic filamentation of the pump and the scattered beams, within the paraxial ray approximations. We have examined that the pump depletion and relativistic filamentation affects the back-reflectivity of scattered beams significantly, for the 5WI case. Due to this filamentation effect, the intensity of the laser beam gets enhanced, which further modifies the gains (g_R and g_B) and consequently the back reflectivity (R_{SRS} and R_{SBS}) also gets enhanced. We have also demonstrated that the back reflectivities (R_{SRS} and R_{SBS}) get suppressed in the coexistence (5WI) case.

ACKNOWLEDGMENT

This work was partially supported by CSIR, India and DST, India.

REFERENCES

Akhmanov, A., Sukhorukov, A.P. & Khokhlov, R.V. (1968). Self-focusing and diffraction of light in a nonlinear medium. *Soviet Phys. Uspekhi* **10**, 609.

Barr, H.C., Berwick, S.J. & Mason, P. (1998). Six-wave forward scattering of short-pulse laser light at relativistic intensities. *Phys. Rev. Lett.* **81**, 2910.

Borghesi, M., Mackinnon, A.J., Barringer, L., Gaillard, R., Gizzi, L.A., Meyer, C., Willi, O., Pukhov, A. & Meyer-Ter-Vehn, J.

(1997). Relativistic channeling of a picosecond laser pulse in a near-critical preformed. *Plasma Phys. Rev.* Lett. **78**, 879.

Brandi, H.S., Manus, C., Mainfray, G. & Lehner, T. (1993). Relativistic self-focusing of ultraintense laser pulses in inhomogeneous underdense plasmas. *Phys. Rev. E* **47**, 3780.

Deutsch, C., Furukawa, H., Mima, K., Murukami, M. & Nishihara, K. (1996). Interaction physics of the fast ignitor concept. *Phys. Rev. Lett.***77**, 2483.

Guérin, S., Laval, G., Mora, P., Adam, J.C., Heron, A. & Bendib, A. (1995). Modulational and Raman instabilities in the relativistic regime. *Phys. Plasmas* **2**, 2807.

Guérin, S., Mora, P. & Laval, G. (1998). Parametric instabilities due to relativistic electron mass variation. *Phys. Plasmas* **5**, 376.

Hao, L., Liu, Z.J., Hu, X.Y. & Zheng, C.Y. (2013). Competition between the stimulated Raman and Brillouin scattering under the strong damping condition. *Laser Part. Beams* **31**, 203.

Kolber, T., Rozmus, W. & Tikhonchuk, V.T. (1995). Saturation of backward stimulated Raman scattering and enhancement of laser light scattering in plasmas. *Phys. Plasmas* **2**, 256.

Krall, N.A. & Trivelpiece, A.W. (1973). *Principles of Plasma Physics*. New York: McGraw-Hill.

Kruer, W.L. (1974). *The Physics of Laser Plasma Interaction*. New York: Addison-Wesley.

Labaune, C., Baldis, H.A., Renard, N., Schifano, E. & Michard, A. (1997). Interplay between ion acoustic waves and electron plasma waves associated with stimulated Brillouin and Raman scattering. *Phys. Plasmas* **4**, 423.

Li, X.Y., Wang, J.X., Zhu, W.J., Ye, Y., Li, J. & Yu, Y. (2011). Enhanced inner-shell x-ray emission by femtosecond-laser irradiation of solid cone targets. *Phys. Rev. E* **83**, 046404.

Lindl, J.D., Amendt, P., Berger, R.L., Glendining, S.G., Glenzer, S.H., Hann, S.W., Kauffman, R.L., Landen, O.L. & Suter, L. (2004). The physics basis for ignition using indirect-drive targets on the National Ignition Facility. *Phys. Plasmas* **11**, 339.

Liu, C.S. & Tripathri, V.K. (1994). *Interaction of Electromagnetic waves with Electron beams and Plasmas*. Singapore: World Scientific.

Mahmoud, S.T. & Sharma, R.P. (2001). Effect of pump depletion and self-focusing (hot spot) on stimulated Raman scattering in laser-plasma interaction. *Laser Part. Beams* **64**, 613.

Michel, D.T., Depierreux, S., Stenz, C., Tassin, V. & Labaune, C. (2010). Exploring the saturation levels of stimulated raman scattering in the absolute regime. *Phys. Rev. Lett.* **104**, 255001.

Monot, P., Auguste, T., Gibbon, P., Jakober, F., Mainfray, G., Dulieu, A., Louis-Jacquet, M., Malka, G. & Miquel, J.L. (1995). Experimental demonstration of relativistic self-channeling of a multiterawatt laser pulse in an underdense plasma. *Phys. Rev. Lett.* **74**, 2953.

Omatsu, T., Kong, H.J., Park, S., Cha, S., Yoshida, H., Tsubakimoto, K., Fujita, H., Miyanaga, N., Nakatsuka, M., Wang, Y., Lu, Z., Zheng, Z., Zhang, Y., Kalal, M., Slezak, O., Ashihara, M., Yoshino, T., Hayashi, K., Tokizane, Y., Okida, M., Miyamoto, K., Toyoda, K., Grabar, A.A., Kabir, M.M., Oishi, Y., Suzuki, H., Kannari, F., Schaefer, C., Pandiri, K.R., Katsuragawa, M., Wang, Y.L., Lu, Z.W., Wang, S.Y., Zheng, Z.X., He, W.M., Lin, D.Y., Hasi, W.L.J., Guo, X.Y., Lu, H.H., Fu, M.L., Gong, S., Geng, X.Z., Sharma, R.P., Sharma, P., Rajput, S., Bhardwaj, A.K., Zhu, C.Y. & Gao, W. (2012). The current trends in SBS and phase conjugation. *Laser Part. Beams* **30**, 117.

Paknezhad, A. (2012). Effect of relativistic nonlinearity on the growth rate of Brillouin instability in the interaction of a short laser pulse with an underdense plasma. *Phys. Scr.* **86**, 065402.

Remington, B.A., Drake, R.P., Takabe, H. & Arnett, D. (1999). Modeling astrophysical phenomena in the laboratory with intense lasers. *Sci.* **284**, 1488.

Rousseaux, C., Le Gloahec, M.R., Baton, S.D., Amiranoff, F., Fuchs, J., Gremillet, L., Adam, J.C., Héron, A. & Mora, P. (2002). Strong absorption, intense forward-Raman scattering and relativistic electrons driven by a short, high intensity laser pulse through moderately underdense plasmas. *Phys. Plasmas* **9**, 4261.

Sharma, R.P., Vyas, A. & Singh, R.K. (2013). Effect of laser beam filamentation on coexisting stimulated Raman and Brillouin Scattering. *Phys. Plasmas* **20**, 102108.

Shuller, S. & Porzio, A. (2010). Order statistics and extreme properties of spatially smoothed laser beams in laser-plasma interaction. *Laser Part. Beams* **28**, 463.

Sprangle, P., Tang, C. & Esarey, E. (1987). Relativistic Self-Focusing of Short-Pulse Radiation Beams in Plasmas. IEEE Trans. *Plasma Sci.* **PS-15**, 145.

Sun, G., Ott, E., Lee, Y.C. & Guzdar, P. (1987). Self-focusing of short intense pulses in plasmas. *Phys. Fluids* **30**, 526.

Tajima, T. & Dawson, J.M. (1979). Laser Electron Accelerator. *Phys. Rev. Lett.* **43**, 267.

Tajima, T. & Mourou, G. (2002). Zettawatt-exawatt lasers and their applications in ultrastrong-field physics. *Phys. Rev. ST* **5**, 031301.

Turnbull, D., Li, S., Morozov, A. & Suckewer, S. (2012). Simultaneous stimulated Raman, Brillouin, and electron-acoustic scattering reveals a potential saturation mechanism in Raman plasma amplifiers. *Phys. Plasmas* **19**, 083109.

Umstadter, D. (2003). Relativistic laser-plasma interactions. *J. Phys. D: Appl. Phys.* **36**, R151.

Walsh, C.J., Villeneuve D, M. & Baldis, H.A. (1984). electron plasma-wave production by stimulated Raman scattering: Competition with stimulated Brillouin scattering. *Phys. Rev. Lett.* **53**, 1445.

Wang, X., Krishnan, M., Saleh, N., Wang, H. & Umstadter, D. (2000). Electron acceleration and the propagation of ultrashort high-intensity laser pulses in plasmas. *Phys. Rev. Lett.* **84**, 5324.

Weber, S., Riconda, C., Lancia, L., Marquès, J.R., Mourou, G.A. & Fuchs, J. (2013). Amplification of ultrashort laser pulses by brillouin backscattering in plasmas. *Phys. Rev. Lett.* **111**, 055004.